

Ca and Be substitution in bulk MgO: 'ab initio' Hartree-Fock and ionic model supercell calculations

This article has been downloaded from IOPscience. Please scroll down to see the full text article.

1993 J. Phys.: Condens. Matter 5 4793

(<http://iopscience.iop.org/0953-8984/5/27/024>)

View [the table of contents for this issue](#), or go to the [journal homepage](#) for more

Download details:

IP Address: 171.66.16.159

The article was downloaded on 12/05/2010 at 14:11

Please note that [terms and conditions apply](#).

Ca and Be substitution in bulk MgO: 'ab initio' Hartree–Fock and ionic model supercell calculations

C Freyria-Fava†, F Dovesi†, V R Saunders‡, M Leslie‡ and C Roetti†

† Department of Inorganic, Physical and Materials Chemistry, University of Torino, Via Giuria 5, I-10125 Torino, Italy

‡ SERC Daresbury Laboratory, Daresbury, Warrington WA4 4AD, UK

Received 30 October 1992, in final form 16 February 1993

Abstract. Be and Ca substitutional impurities in bulk MgO are studied using the periodic *ab initio* Hartree–Fock method and the considerably simpler ionic model based on two-body forces and the dipole shell model. In both cases a supercell approach was used; in the Hartree–Fock calculations the largest unit cell contained 32 atoms whilst in the case of the ionic model supercells of up to 250 atoms were employed. The Hartree–Fock results for the Be and Ca defect formation energies are -4.10 and 6.25 eV respectively, the corresponding results from the ionic model being -3.88 and 6.37 eV, these data being defined with respect to ionic, rather than atomic, substitutions. The effect of such defects on the Hartree–Fock charge distribution of the host is examined in terms of nuclear displacements (these being compared with the corresponding results of the ionic model) and electronic redistribution, the latter being analysed in terms of charge density maps and induced atomic multipoles. The convergence pattern of the Hartree–Fock defect formation energies is discussed using data from cells containing 8, 16 and 32 atoms. The larger unit cells employed with the ionic model allow a more careful study of the convergence rate of the supercell method.

1. Introduction

Numerous techniques have been proposed for the quantum-mechanical study of local defects in solids [1]. Cluster and supercell approaches are the most widely used, because they exploit in a straightforward way the tools implemented in molecular quantum chemistry and band structure 'total energy' calculations respectively. The main difficulty of the supercell scheme is related to the interaction of defects located in neighbouring cells. For charged defects in particular it is necessary to restore the electroneutrality of the unit cell with a compensating uniform background charge, and to correct the defect formation energy using an estimate of the dielectric response of the host system to the periodic ensemble of neutralized defects [2].

In the present work we apply the supercell approach within the Hartree–Fock LCAO formalism as implemented in the program CRYSTAL [3] to the study of the substitution of an Mg atom by either a Be or a Ca atom in the rock-salt structure MgO. Those systems have been investigated in previous studies using the ionic model with two-body potentials [4]. Such ionic model studies, again using a supercell approach, have been extended in the present work using the program SYMLAT [5], thereby allowing a detailed comparison of the results of the Hartree–Fock and ionic models. We will investigate:

- the numerical accuracy of the CRYSTAL program in large-unit-cell calculations, the scale of energy of interest being a typical defect formation energy (ΔE)

- the trend of the cost with increasing size of the unit cell
- the convergence of the defect energy and wavefunction as a function of the unit cell size, and
- the number of atoms involved in the relaxation process.

2. Computational details

The ionic model calculations use O–O, Mg–O and Ca–O short-range potentials due to Sangster and Stoneham [6]. The Be–O short-range potential is of the form $Ae^{-r/\rho}$, where $A = 1126.75$ eV and $\rho = 0.2791$ Å, and has been derived from a potential due to Walker reported on page 114 of [7], which is applicable to four-coordinated Be, by scaling according to the ionic radii of four- and six-coordinated Be (0.27 and 0.35 Å respectively) given by Shannon and Prewitt [8]. The dipole shell model for the anion is from [6].

Hartree–Fock calculations have been carried out using the Gaussian basis sets reported in the appendix (see table A1). The host system's bulk properties have been investigated with the same basis sets [9]. Similar all-electron studies of CaO [10] and BeO [11] are at an advanced stage. A selection of calculated and experimental bulk properties of MgO, CaO and BeO are given in the appendix (see table A2).

Table 1. Total Hartree–Fock energy per MgO unit (E_{tot}) and cost of the calculation for bulk MgO as a function of the unit cell size. M is the number of atoms per unit cell; N_i is the number (10^6 units) of bi-electronic integrals evaluated; N_s is the number (10^6 units) of symmetrized sums of bi-electronic integrals stored for the SCF iterations. t_1 and t_2 give the CPU seconds (on an IBM 9121 computer) required for the integral evaluation and SCF parts of the calculation respectively. is is the shrinking factor of the reciprocal lattice net; N_k is the number of k points at which the Fock matrix is diagonalized. NCY is the number of SCF cycles necessary to obtain convergence of the total energy to 10^{-5} Hartree.

M	N_i	N_s	t_1	is	N_k	NCY	t_2	E_{tot}
2	37.5	0.3	85	8	29	6	8	-274.66437
8	91.5	1.8	289	4	10	6	54	-274.66437
16	129.5	3.8	541	4	8	6	357	-274.66437
32	191.6	8.7	1138	2	3	6	462	-274.66437

Let us consider some of the problems connected with the size of the supercell. In table 1 the total energy and the cost of the Hartree–Fock calculations for cells containing one, four, eight and 16 MgO units are reported. These data show that the total energy per MgO unit is constant to five decimal places. This is apparently obvious, as the same basis sets and geometry have been used in all the calculations. In practice the four calculations are very different from many points of view: the number of integrals to be evaluated, the dimensions of the matrices to be diagonalized etc., so table 1 indicates that the numerical accuracy and stability of the CRYSTAL program is reassuringly high. It is of interest to consider the trend of the cost of the calculations in the integral evaluation (t_1) and SCF (t_2) parts. t_1 increases approximately linearly with the number of atoms in the unit cell. It appears that calculations with up to say 128 atom unit cells should be feasible (costing an estimated 80 min). As regards t_2 , it is directly proportional to the number of sampling k points in the first Brillouin zone (N_k) as well as to the number of iterative cycles. The increase in t_2 with unit cell size is not too rapid simply because the third-power increase in diagonalization time is partially balanced by the decrease of N_k , the latter being justified by the increase in the unit cell

size. It must be noticed that, in order to have exactly the same accuracy in the reciprocal space numerical integration for calculating the density matrix, one should divide by two the shrinking factor, $1S$, when the cell edge is doubled; this is the reason why $1S$ is reduced as the size of the unit cell increases. With the present structure of the code, $1S$ cannot be smaller than two (corresponding to a maximum of eight irreducible k points). We estimate t_2 to be of the order of 400 min for a 128-atom unit cell, which would be reduced by approximately one order of magnitude on a CRAY Y-MP machine, as this part of code is well vectorized.

It is to be noticed that we are here using CRYSTAL for a supercell option in a 'brute force' way. Many improvements based on exploiting the regular behaviour of supercell calculations are possible which would considerably reduce the cost of the calculations.

3. Results and discussion

The principal effect to be expected from the substitution of an Mg with a Ca or Be ion in bulk MgO is the relaxation of the lattice around the defect, due to the different sizes of the cations. The experimental Ca-O (rock-salt structure—sixfold coordination) and Be-O (wurtzite structure—fourfold coordination) distances are 2.40 and 1.64 Å respectively, to be compared with 2.10 Å in MgO.

Table 2. Ca^{2+} and Be^{2+} Hartree-Fock substitutional energies (ΔE in eV) in MgO for the 32-atom supercell as a function of the number of stars of neighbours which are allowed to relax. 'Second' means that the first and second neighbours have been allowed to relax. ΔR is the variation (in Å) of the distance between the defect and its first (six O) and second (12 Mg) neighbours. These distances are 2.105 and 2.977 Å respectively in the perfect MgO crystal.

Case	Ca			Be		
	ΔE	ΔR		ΔE	ΔR	
		O	Mg		O	Mg
unrelaxed	7.09	—	—	-3.83	—	—
first	6.44	0.084	—	-4.00	-0.053	—
second	6.25	0.097	0.031	-4.10	-0.070	-0.022

In the present Hartree-Fock calculations, three situations have been considered: the unrelaxed structure (entitled 'unrelaxed' in table 2) and the situations where nearest neighbours and next-nearest neighbours (entitled 'first' and 'second' respectively in table 2) are allowed to relax. The substitutional defect formation energy refers to ionic limits, and has been evaluated according to the equation

$$\Delta E_X = E_{\text{MgO-X}} - N E_{\text{MgO}} + E_{\text{Mg}^{2+}} - E_{\text{X}^{2+}} \quad (1)$$

where $E_{\text{MgO-X}}$ is the total energy per supercell of the defective structure, N is the number of MgO units in the corresponding perfect lattice supercell, E_{MgO} is the energy of the bulk MgO per MgO unit, while $E_{\text{Mg}^{2+}}$ and $E_{\text{X}^{2+}}$ denote the total energies of the isolated ions. An equivalent expression can be given in terms of the isolated atoms:

$$\Delta E'_X = E_{\text{MgO-X}} - N E_{\text{MgO}} + E_{\text{Mg}} - E_{\text{X}} \quad (2)$$

In the appendix the calculated Hartree-Fock atomic and ionic energies are reported (see table A3) whence it can be deduced that:

$$\Delta E'_{\text{Be}} = \Delta E_{\text{Be}} + 5.01 \text{ eV} \quad (3)$$

$$\Delta E'_{\text{Ca}} = \Delta E_{\text{Ca}} - 4.72 \text{ eV}. \quad (4)$$

Table 2 shows that the Ca substitutional energy reduces from 7.09 eV to 6.44 eV when the first star of neighbours (six O ions) is allowed to relax; a further energy gain of 0.19 eV is obtained after allowing the second neighbours (12 Mg ions) to relax, the total relaxation energy, 0.84 eV, being substantial. In the case of the Be substitution, the relaxation energy, 0.27 eV, is considerably smaller. In the Be case the displacements are smaller and in the opposite direction to those for the Ca substitution, but the pattern is otherwise qualitatively similar. It is of interest to consider the relative importance of the electronic rearrangement and nuclear displacement in response to the defect formation, and the distance to which these effects propagate. Some light is thrown on this question by the data of table 3, where it is shown that ΔE for the unrelaxed defect in a supercell with eight, 16 and 32 atoms is essentially invariant. A similar pattern is observed for the 16- and 32-atom unit cells when the first star of neighbours is allowed to relax. Quite small unit cells appear to be able to describe the effect of electronic rearrangement. In contrast, table 2 indicates that nuclear positional relaxation is much more long ranged, at least for fully ionic compounds such as MgO. Further information on this matter is given by the data of table 4 pertaining to the ionic model calculations, where the defect formation energies and ionic relaxation up to the fourth star of neighbours are recorded for supercells of up to 250 atoms. The convergence pattern of the ionic model ΔE and ΔR data is very similar to that of the Hartree-Fock results for the eight-, 16- and 32-atom unit cells, confirming that the ionic model is able to provide accurate formation energies and relaxation geometries. Nuclear displacements of up to fourth neighbours are appreciable. Nevertheless, the energetic effect of nuclear displacements beyond second neighbours is relatively small, so that the use of 32-atom supercell causes the defect formation energy to be not more than 0.1 eV greater than that found from asymptotically large supercells.

Table 3. Ca^{2+} and Be^{2+} Hartree-Fock substitutional energies (ΔE in eV) in MgO as a function of the size of the supercell. M is the number of atoms in the supercell. ΔR is as in table 2.

M	Ca			Be		
	ΔE	ΔR		ΔE	ΔR	
		O	Mg		O	Mg
8	7.20	—	—	-3.81	—	—
16	7.12	—	—	-3.80	—	—
32	7.09	—	—	-3.83	—	—
16	6.56	0.073	—	-3.93	-0.044	—
32	6.43	0.084	—	-4.00	-0.053	—
32	6.25	0.097	0.031	-4.10	-0.070	-0.022

Further information is provided by the atomic charges (q), dipoles (μ) quadruples (Q) and 'spheropoles' (r square root of the spherical second-order moment) evaluated using a Mulliken partitioning of the charge distribution (see table 5) and according to the definitions

Table 4. Ca^{2+} and Be^{2+} ionic model substitutional energies (ΔE in eV) in MgO as a function of size of the supercell. ΔR is as in table 2, with the third (eight O) and fourth (six Mg) neighbours at 3.646 Å and 4.210 Å respectively from the defect position in the perfect MgO crystal. M is as in table 3.

M	Ca					Be				
	ΔE	ΔR				ΔE	ΔR			
		First	Second	Third	Fourth		First	Second	Third	Fourth
8	7.45	—	—	—	—	-3.36	—	—	—	—
16	6.79	0.083	—	—	—	-3.64	-0.064	—	—	—
32	6.47	0.107	0.038	—	—	-3.83	-0.095	-0.031	—	—
54	6.47	0.109	0.030	-0.000	0.006	-3.82	-0.093	-0.027	0.002	0.003
64	6.40	0.113	0.039	-0.010	—	-3.87	-0.100	-0.034	0.006	—
128	6.39	0.117	0.038	-0.009	0.017	-3.87	-0.100	-0.034	0.005	-0.001
250	6.37	0.120	0.042	-0.008	0.022	-3.88	-0.102	-0.036	0.005	-0.003

Table 5. Net atomic charges (q), dipole (μ), quadrupole (Q) and spheropole (r) moments for the Ca and Be substitution in MgO, in atomic units. The sign convention of the dipole and quadrupole moments is explained in the text. The oxygen spheropole moment in perfect MgO is 4.391 bohr.

Atom	Unrelaxed				First				Second			
	Q	μ	Q	r	q	μ	Q	r	q	μ	Q	r
Ca	1.984	0.0	0.0	3.625	1.906	0.0	0.0	3.781	1.920	0.0	0.0	3.779
O ₁	-1.979	0.171	0.446	4.347	-1.972	0.044	0.381	4.349	-1.967	0.034	0.389	4.354
O ₃	-1.980	0.0	-0.009	4.391	-1.980	0.0	-0.051	4.392	-1.980	0.0	-0.046	4.392
Be	1.861	0.0	0.0	0.930	1.865	0.0	0.0	0.923	1.868	0.0	0.0	0.917
O ₁	-1.960	-0.067	-0.199	4.402	-1.955	0.005	-0.175	4.392	-1.947	0.039	-0.152	4.390
O ₃	-1.979	0.0	0.005	4.391	-1.979	0.0	0.026	4.392	-1.979	0.0	0.040	4.392

Table 6. Atomic orbital populations on the two outermost (valence) shells of the first-neighbour O atoms. The p_z orbital points towards the defect. The oxygen basis set is given in table A1.

Substitution	Shell	Unrelaxed		First		Second	
		$p_x = p_y$	p_z	$p_x = p_y$	p_z	$p_x = p_y$	p_z
Ca	inner	1.133	1.186	1.135	1.183	1.133	1.182
	outer	0.855	0.813	0.852	0.810	0.853	0.812
Be	inner	1.157	1.110	1.156	1.112	1.154	1.111
	outer	0.835	0.864	0.834	0.860	0.834	0.858

of [12]. The Mg ions exhibit so little perturbation under defect formation, their charge remaining essentially at the bulk MgO value (see table A2), while the induced multipole moments are negligible, that we have not thought it worthwhile to incorporate the relevant data into table 5. The defect atoms themselves appear to be more ionic than in bulk CaO and BeO (compare with table A2). This is probably because of the stronger Madelung potentials encountered in MgO, due to the larger lattice constant of CaO and the lowering of the coordination number to four on passing to BeO. As is to be expected, the anions exhibit the largest perturbation, and table 5 summarizes the effects for the first and third

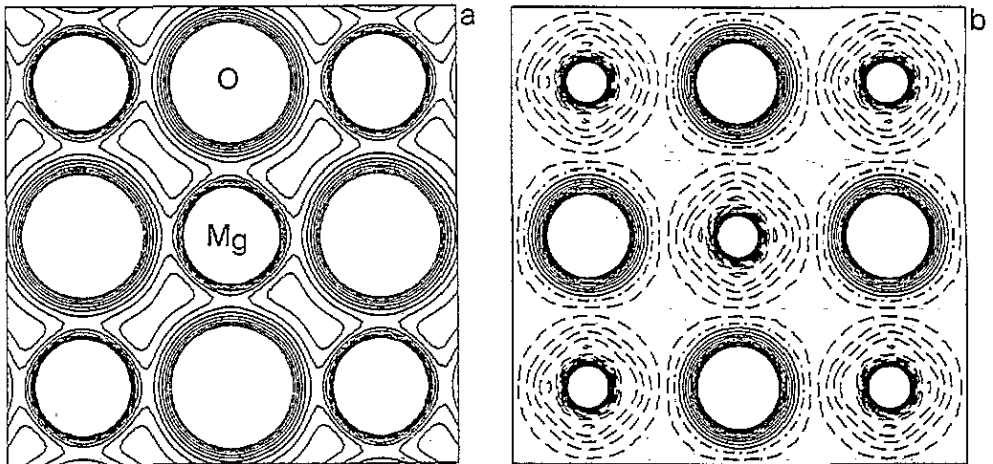


Figure 1. Total (a) and difference (b) charge density maps for bulk MgO. The section is parallel to the (001) plane. Contour intervals of 0.01 and 0.001 e bohr³ for total and difference maps respectively (lowest contour interval at 0.02 e bohr³). Full, broken and chain curves correspond to positive, negative and null values, respectively.

stars of neighbours with respect to the defect (labelled O₁ and O₃ respectively; recall that Mg ions lie at the second-neighbour positions). For both stars of neighbours the dipoles are always oriented along the line connecting the neighbour to the defect, and we have adopted the convention that positive and negative dipoles point towards or away from the defect respectively. Thus a positive dipole corresponds to the electrons of the anion drifting away from the defect. With respect to the quadrupole tensor the anion charge clouds behave as ellipsoids whose axis of rotation is the line connecting the anion to the defect. In this principal axis system the quadrupole tensor is of the form:

$$Q \begin{pmatrix} 1 & 0 & 0 \\ 0 & -\frac{1}{2} & 0 \\ 0 & 0 & -\frac{1}{2} \end{pmatrix}$$

where Q is positive or negative for oblate or prolate electronic charge clouds respectively. In the unrelaxed calculations a large dipole is induced on the first-neighbour O atoms, pointing towards and away from the Ca and Be defects respectively (electrons are repelled from the Ca, but attracted towards the Be, as would be expected from considerations of the ionic radii). After nuclear relaxation this dipole is greatly reduced; the nuclei tend to 'follow' their electrons, becoming the baricentres of their respective charge clouds. Such features are also quite evident in figures 2 and 3 (in figure 1 total and difference charge density maps of the perfect crystal are reported for comparison). The large quadrupole induced on the first-neighbour O (oblate and prolate for Ca and Be substitution respectively, again in accordance with our ideas concerning the effects of ionic radii), is, however, only slightly reduced by relaxation. The first-neighbour O quadrupole moment in the Ca substituted system arises because electrons in the outer O P_z valence orbital (the z axis is the line connecting the defect to its first neighbour) are transferred to the inner p_z valence orbital (note from table A1 that the O basis set includes two valence sp shells) in order to reduce short-range repulsion with the Ca ion. Electrons in the p_x, p_y orbitals transfer from the inner to the outer shells to reduce the electronic repulsion with the p_z electrons (see table 6). Thus, near the O

nucleus the polarization is prolate, becoming oblate at longer range. Careful examination of figure 2(c) shows the inner prolate structure of the O charge distribution, tending to oblate at larger distances. Ca substitution causes the first-neighbour O ions to spherically contract as can be seen from the spheropole moments, r , quoted in table 5. Analogous but reversed first-neighbour O ion quadrupolar relaxation and spherical breathing occurs in the Be substitution case, but with a considerably reduced magnitude (see table 5 and figure 3(c)).

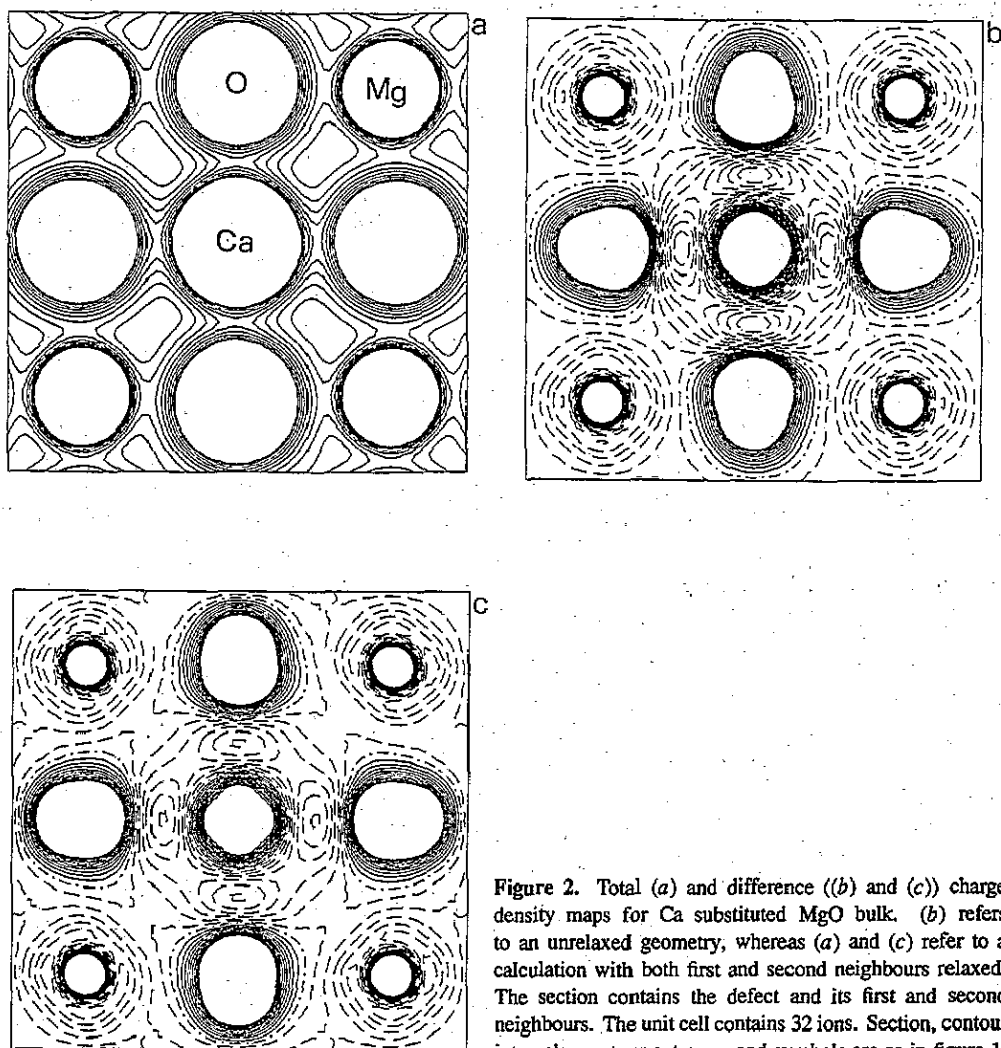


Figure 2. Total (a) and difference ((b) and (c)) charge density maps for Ca substituted MgO bulk. (b) refers to an unrelaxed geometry, whereas (a) and (c) refer to a calculation with both first and second neighbours relaxed. The section contains the defect and its first and second neighbours. The unit cell contains 32 ions. Section, contour intervals, contour extremes and symbols are as in figure 1.

4. Conclusions

The present work has demonstrated that the application of the periodic Hartree-Fock method to neutral defects is feasible using relatively large supercells. The convergence of the results

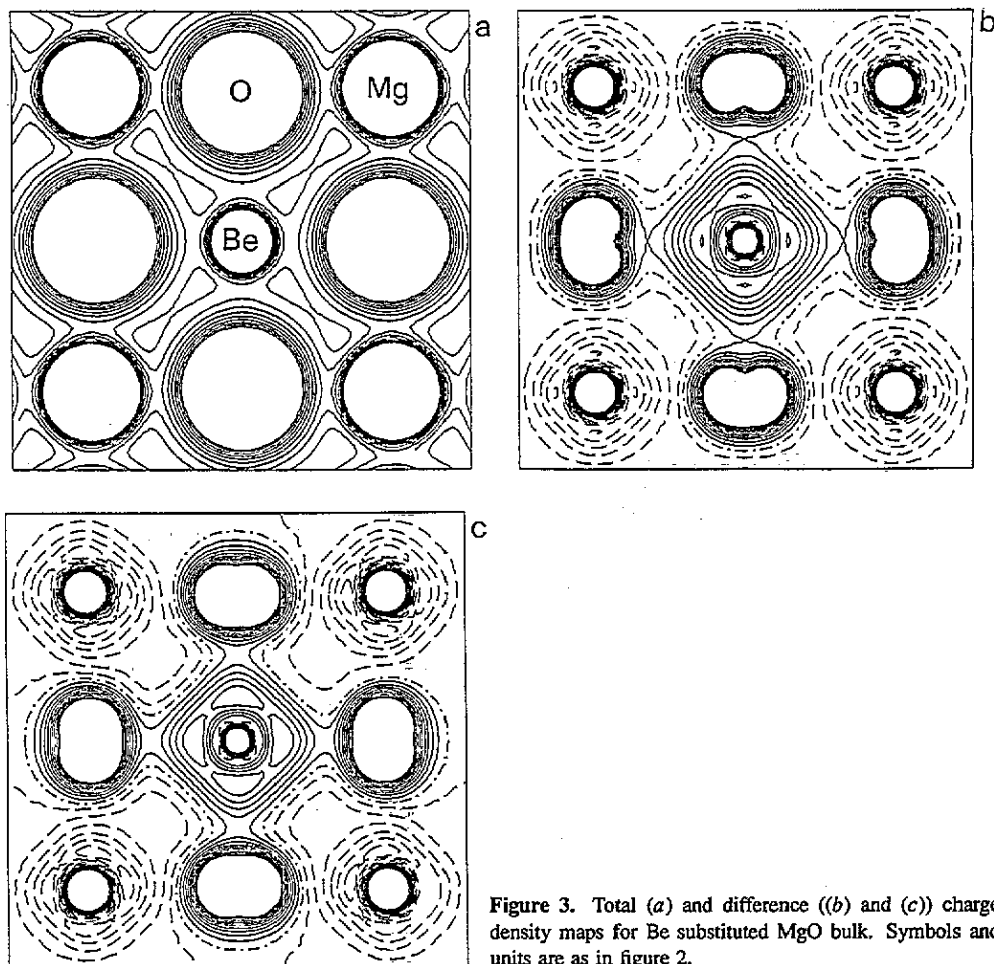


Figure 3. Total (*a*) and difference (*b*) and (*c*) charge density maps for Be substituted MgO bulk. Symbols and units are as in figure 2.

with respect to supercell size has been shown to be satisfactory and consistent with similar data produced from ionic model calculations in the case of Ca and Be substitutional defects in MgO. The Hartree–Fock model provides a wealth of information regarding electronic relaxation processes accompanying defect formation. In particular it turns out that the defect substantially modifies the electronic structure of the first-neighbour O atoms, not only through dipolar deformation (which is also accounted for in the ionic model program SYMLAT [5] through the dipole shell model [13]) but also through spherical breathing and quadrupolar deformations. The latter two mechanisms are not accounted for in SYMLAT [5], which however gives energy and geometric relaxation data in good agreement with those of the quantum-mechanical calculations; we are unable to tell whether such agreement is merely fortuitous, or implies that the quadrupolar and spherical breathing mechanisms are energetically unimportant. The consistency of the trends reported above and the many reliable defect energies and atomic relaxations provided by the ionic model for ionic and semi-ionic compounds [4–6] seem to favour the second hypothesis; however an unambiguous resolution of the question would require the introduction of reasonable models of both quadrupolar deformation [14] and spherical breathing mechanisms [15] into the SYMLAT calculations.

Table A1. Exponents (bohr⁻²) and coefficients of the Gaussian basis sets used for the four atoms of interest in the present work: Be, Mg, Ca and O. The coefficients refer to individually normalized Gaussians.

Atom	Shell		Exponent	Coefficients		
	Number	Type		s	p	d
Be	2	s	1670.0	0.00241	—	—
			343.4	0.0085	—	—
			121.1	0.0341	—	—
			32.13	0.1849	—	—
			8.322	0.6419	—	—
	2	sp	2.335	1.0	1.0	—
Mg	3	sp	0.664	1.0	1.0	—
	1	s	68372.0	0.0002226	—	—
			9699.3	0.0018982	—	—
			2041.2	0.011045	—	—
			529.86	0.050063	—	—
			159.19	0.16912	—	—
			54.685	0.36703	—	—
			21.236	0.40041	—	—
			8.746	0.14987	—	—
	2	sp	156.79	-0.00624	0.00772	—
			31.034	-0.07882	0.06427	—
			9.6453	-0.07992	0.02104	—
			3.7109	0.29063	0.34314	—
1.6116			0.57164	0.3735	—	
0.64294			0.30664	0.23286	—	
Ca	3	sp	0.4	1.0	1.0	—
	1	s	191300.0	0.0002204	—	—
			26970.0	0.001925	—	—
			5696.0	0.01109	—	—
			1489.4	0.04995	—	—
			448.3	0.17014	—	—
			154.62	0.3685	—	—
			60.37	0.4034	—	—
			2.509	0.1452	—	—
	2	sp	448.6	-0.00575	0.00847	—
			105.7	-0.0767	0.06027	—
			34.69	-0.1122	0.2124	—
			13.5	0.2537	0.3771	—
5.82			0.688	0.401	—	
1.819			0.349	0.198	—	
3	sp	20.75	-0.002	-0.0365	—	
		8.4	-0.1255	-0.0685	—	
		3.597	-0.696	0.157	—	
		1.408	1.029	1.482	—	
		0.726	0.944	1.025	—	

Appendix

In table A1 the basis sets of the four ions involved in the present calculation are reported. The bases adopted for Mg and O are as in the study of MgO bulk [9]; the bases for Be and Ca are as used in the study of BeO [11] and CaO [10]. In those two studies a slightly larger basis set has been used for O: 8-5-11 G instead of the contraction 8-6-1 G of table A1.

Table A1. (continued)

Atom	Shell			Coefficients			
	Number	Type	Exponent	s	p	d	
	4	sp	0.453	1.0	1.0	—	
	5	sp	0.246	1.0	1.0	—	
	6	d	3.922	—	—	0.139	
			1.095	—	—	0.326	
			0.38	—	—	0.427	
	O	1	s	4000.0	0.00144	—	—
				1355.6	0.00764	—	—
				248.54	0.0537	—	—
				69.534	0.16818	—	—
				23.887	0.36039	—	—
9.2759				0.38612	—	—	
3.8203				0.14712	—	—	
1.2351				0.07105	—	—	
2		sp	52.188	-0.00873	0.00922	—	
			10.329	-0.08979	0.07068	—	
			3.2103	-0.04079	0.20433	—	
			1.2351	0.37666	0.34958	—	
			0.53642	0.42248	0.27774	—	
3		sp	0.21	1.0	1.0	—	

Table A2. Calculated and experimental bulk properties of BeO, MgO and CaO. E_{tot} (Hartree) is the total energy per XO unit, BE (Hartree) the binding energy, R_{XO} (Å) the cation-oxygen distance, B (GPa) the bulk modulus, q the ionic net charge from a Mulliken analysis. The calculated BeO data refer to the zinc-blende structure (zB, space group $F\bar{4}3m$), whereas the experimental results refer to the wurtzite structure (W, space group $P6_3mc$). Note however that from the calculation it turns out that the differences (zB minus W) between the two structures for E_{tot} , R_{XO} and B are very small: 0.002 Hartree (the W structure is more stable than the zB structure), 0.02 Å and -2 GPa, respectively. MgO and CaO data refer to the rock-salt structure.

E_{tot}	BE		R_{XO}		B		q
	Calculation	Experiment	Calculation	Experiment	Calculation	Experiment	
BeO - 89.6937	0.340	0.446	1.64	1.64	239	220	1.75
MgO -274.6644	0.283	0.376	2.10	2.10	186	167	1.98
CaO -751.7923	0.283	0.399	2.42	2.40	128	123	1.80

The formation energy, equilibrium lattice parameter (a_0) and bulk modulus (B) obtained with the basis sets of table A1 are reported in table A2. Two extra (diffuse) sp shells have been added to the basis set of table A1 in the isolated atom calculations (only one in the case of O) in order to better describe the valence wavefunction. In the case of the isolated ions, one extra shell has been added (none for Mg^{2+}). This additional variation freedom is supposed to allow the isolated species to become more diffuse than in the bulk, and to correct for the basis set superposition error [16]. The exponents of the added functions and of the most diffuse shell of the bulk basis (table A1) have been optimized, and are reported in table A3. The defect formation energy of the 32-atom unit cell can be evaluated from atoms and ions using tables A2 and A3 after taking into account that the total energy of the 32-atom substituted cell is -4871.702384 Hartree (Ca) and -4209.568647 (Be) (case entitled 'second' in table 2), by using equations (1) and (2) and the perfect crystal

Table A3. Exponents (bohr⁻²) of the most diffuse sp shells used for the evaluation of the atomic and ionic energies of Be, Mg, Ca and O. α_1 is the reoptimized exponent of the most diffuse shell of table A1; α_2 and α_3 refer to the two sp shells added to take into account the tails of the atomic wavefunction. The cation energies have been evaluated after adding to the atomic basis set of table A1 one (none in the Mg²⁺ case) extra sp shell.

	Exponents			E_{tot}	E_{kin}
	α_1	α_2	α_3		
Be	0.664	0.244	0.069	-14.5695	14.5695
Mg	0.280	0.073	0.023	-199.5972	199.5393
Ca	0.338	0.118	0.036	-676.7258	676.6384
O	0.202	0.087	—	-74.7839	74.9340
Be ²⁺	0.664	0.400	—	-13.6085	13.6029
Mg ²⁺	0.136	—	—	-198.8204	198.6868
Ca ²⁺	0.368	0.181	—	-676.1226	676.0565

energies of table 1. Table A2 shows that the Hartree-Fock method and the present basis sets reproduce very accurately the BeO and MgO lattice parameters; in the CaO case the present method gives an overestimation of about 1.2% due to the large polarizability of the Ca²⁺ cation, with a consequent increase in importance of dispersion effects, not taken into account at the Hartree-Fock level; a (very small) overestimation of the Ca-O₁ distance in the defective solid is therefore to be expected. The bulk moduli are overestimated by about 10%; the binding energy is underestimated by about 0.1 Hartree/cell in the three cases. This error is mainly due to the difference in correlation energy of the ionic pairs X²⁺O²⁻ (X = Be, Mg, Ca) of the bulk and the neutral isolated atoms X and O; this can be confirmed by evaluating the difference in correlation energy between the isolated ions and atoms; we suppose that in the bulk the modification of the ions (contraction) has a minor effect on the correlation energy difference. The numbers from the data of Clementi [17], are $\Delta E_{\text{corr}} = +0.043$ and -0.147 Hartree for Be²⁺/Be and O²⁻/O respectively, where the result for O²⁻/O has been obtained by extrapolating the data from the isoelectronic series Ne/Ne²⁺, F⁻/F⁺; ΔE_{corr} for Mg²⁺/Mg and Ca²⁺/Ca is very close to that for Be²⁺/Be. In the evaluation of the defect energy, equation (1), it is reasonable to suppose that correlation effects largely cancel because every atom of the reagents and products is essentially at the ionic limit. The defect energy, equation (2), is also largely unaffected by correlation effects because the correlation energy difference of the cation/metal pairs is very similar for the three metals involved.

References

- [1] Pisani C, Orlando R and Nada R 1992 *Cluster Models for Surface and Bulk Phenomena* ed G Pacchioni (New York: Plenum)
- [2] Bar-Yam Y and Joannopoulos J D 1984 *Phys. Rev. B* **30** 1844
Leslie M and Gillan M J 1985 *J. Phys. C: Solid State Phys.* **18** 973
Nichols C S, Van de Walle C G and Pantelides S T 1989 *Phys. Rev. B* **40** 5484
- [3] Pisani C, Dovesi R and Roetti C 1988 *Lecture Notes in Chemistry* vol 48 (Heidelberg: Springer)
Dovesi R, Pisani C, Roetti C and Saunders V R 1989 CRYSTAL 88 Program no 577
Quantum Chemistry, Program Exchange, Indiana University
Dovesi R, Saunders V R and Roetti C 1992 *CRYSTAL 92 User's Manual* Università di Torino and SERC Daresbury Laboratory
- [4] Mackrodt W C and Stewart R F 1979 *J. Phys. C: Solid State Phys.* **12** 5015

- Colbourn E A, Mackrodt W C and Tasker P W 1983 *J. Mater. Sci.* **17** 1917
Mackrodt W C 1982 *Lecture Notes in Physics* vol 166 ed C R A Catlow and W C Mackrodt W C (Berlin: Springer) p 187
- [5] Leslie M 1983 *Solid State Ion.* **8** 243
 - [6] Sangster M J L and Stoneham A M 1985 *Phil. Mag.* **B 52** 717
 - [7] Stoneham A M 1979 *Handbook of Interatomic Potentials* AERE R-9598
 - [8] Shannon R D and Prewitt C T 1969 *Acta Crystallogr.* **B 25** 925
 - [9] Causà M, Dovesi R, Pisani C and Roetti C 1986 *Phys. Rev.* **B 33** 1308
 - [10] Stuart J, Price D and Saunders V R in preparation
 - [11] Lichanot A, Chaiffet M, Larrieu C, Dovesi R and Pisani C 1992 *Chem. Phys.* **164** 383
 - [12] Saunders V R, Freyria-Fava C, Dovesi R, Salasco L and Roetti C 1992 *Mol. Phys.* **77** 629
 - [13] Dick G B and Overhauser A W 1958 *Phys. Rev.* **112** 90
 - [14] Fischer K, Biltz H, Haberkorn R and Weber W 1972 *Phys. Status Solidi* **b 54** 285
 - [15] Schroeder U 1966 *Solid State Commun.* **4** 347
 - [16] Boys S F and Bernardi F 1970 *Mol. Phys.* **19** 553
 - [17] Clementi E 1963 *J. Chem. Phys.* **38** 2248